

Transient Heat Transfer Experiment
ME 331 Introduction to Heat Transfer
June 1st, 2017

Abstract

The lumped capacitance assumption for transient conduction was tested for three heated spheres; a gold plated copper sphere, a black painted copper sphere, and a rubber sphere. The assumption was validated for the gold plated copper and the black painted copper spheres and the lumped capacitance method was used to quantify the total heat loss through natural convection and radiation exchange with the surroundings. The measured heat loss was compared to the predicted heat loss from empirical correlations and found to be within 9% for the gold plated copper sphere and within 8% for the black painted copper sphere on average, over the entire time history.

Introduction

The lumped capacitance method for transient conduction analysis is developed under the assumption that the temperature distribution within a solid is spatially uniform during the entire heating or cooling process. From Fourier's law of thermal conductivity, a uniform spatial temperature gradient is not possible for a real system; however, if the internal conduction resistance of the solid is very small compared to the convection and radiation resistances at the surface, the lumped capacitance method provides a reasonable approximation for the temperature throughout the solid at any given time. The Biot number, a dimensionless ratio of the conduction resistance to the convection and radiation resistances at the surface, is used to check the validity of the lumped capacitance method. For a sphere, the Biot number is:

$$Bi = \frac{h \left(\frac{r_o}{3} \right)}{k} \quad (1)$$

where h (W/m²-K) is the effective heat transfer coefficient, r_o (m) is the radius of the sphere, and k is the thermal conductivity of the solid (W/m-K). To calculate the experimental heat transfer coefficient from measured data, the temperature as a function of time is normalized:

$$\frac{\theta}{\theta_i} = \frac{T(t)_{r=0} - T_\infty}{T_i - T_\infty} \quad (2)$$

where $T(t)_{r=0}$ is the measured temperature at the center of the sphere, T_i is the initial temperature at the center of the sphere and T_∞ is the temperature of the surroundings and ambient air. The natural logarithm of the dimensionless temperature ratio in (2) is then plotted as a function of time and the slope of the line tangent to the curve is used to obtain the overall effective heat transfer coefficient, comprised of both convection and radiation heat transfer effects. The lumped capacitance method is valid when the following criteria is satisfied:

$$Bi \ll 0.1 \quad (3)$$

If the Biot number is less than 0.1 and there is no thermal energy generation within the sphere, an energy balance on a lumped control volume yields:

$$q_{total,m} = h_{effective} * A_s * (T - T_{\infty}) = \rho V c \frac{dT}{dt} \quad (4)$$

where $q_{total,m}$ (in Watts) is the measured total heat transfer rate, $h_{effective}$ is the overall effective heat transfer coefficient, A_s is the surface area of the solid, T is the measured temperature as a function of time, T_{∞} is the ambient and surrounding room temperature, ρ (kg/m^3) is the density of the sphere, V (m^3) is the volume of the sphere, c (J/kg-K) is the specific heat of the sphere and dT/dt is the derivative of the measured temperature of the sphere with respect to time. The total predicted heat transfer is the sum of the predicted convection and predicted radiation heat transfer:

$$q_{total,p} = q_{convection,p} + q_{radiation,p} \quad (5)$$

where $q_{total,p}$ (in Watts) is the predicted total heat transfer rate. For natural convection, the empirical heat transfer rate is dependent on the non-dimensional Rayleigh number:

$$Ra_D = \frac{g\beta(T_s - T_{\infty})D^3}{\nu\alpha} \quad (6)$$

where g (m/s^2) is acceleration due to gravity, D (m) is the diameter of the sphere, T_s (K) is the surface temperature, T_{∞} is the temperature of the ambient air and surroundings, ν (m^2/s) is the kinematic viscosity, α (m^2/s) is the thermal diffusivity, and β ($1/\text{K}$) is the volumetric thermal expansion coefficient. For an ideal gas, this is:

$$\beta = \frac{1}{T_f} \quad (7)$$

where T_f is the film temperature:

$$T_f = \frac{T_s + T_{\infty}}{2} \quad (8)$$

The film temperature is calculated from the sphere surface and surrounding air temperatures recorded over the entire time history. All properties for the Rayleigh number and the convection coefficient are evaluated at the film temperature. For spheres in fluids with a Prandtl number greater than or equal to 0.7 and a Rayleigh number equal to or less than 10^{11} , the average Nusselt number correlation from Churchill is recommended:

$$\overline{Nu}_D = 2 + \frac{0.589Ra_D^{1/4}}{\left[1 + \left(\frac{0.469}{Pr}\right)^{9/16}\right]^{4/9}} \quad (9)$$

in which the spatially averaged convection heat transfer coefficient is related to the Nusselt number, diameter of the sphere, and thermal conductivity of the fluid:

$$\bar{h} = \frac{\overline{Nu}_D k_f}{D} \quad (10)$$

This heat transfer coefficient is related to the predicted convection heat transfer rate through Newton's law of cooling:

$$q_{convection,p} = \bar{h}A_s(T_s - T_\infty) \quad (11)$$

where A_s (m^2) is the surface area of the object. The predicted radiation heat transfer rate is calculated from:

$$q_{radiation,p} = \varepsilon\sigma A_s(T_s^4 - T_\infty^4) \quad (12)$$

where ε is the surface emissivity and σ ($W/m^2 \cdot K^4$) is the Stefan-Boltzmann constant.

The experimental system consisted of a temperature controlled hot water bath, a gold plated copper sphere, a black painted copper sphere, a rubber sphere, and a mounting rig for the spheres. Each of the spheres was fitted with a hollow mounting stem and drilled cavity. The hollow stem and drilled cavity allowed a thermocouple to be routed down the stem into the cavity and seated at the center of the volume to record the sphere's core temperature. Additionally, one thermocouple measured the hot water bath temperature and a second thermocouple measured the ambient, surrounding air temperature.

Procedure

The following steps were performed for data collection:

1. The water bath was heated and temperatures were monitored until steady state was reached.
2. Once the hot water bath reached steady state, one of the three spheres was selected and the thermocouple was fed down the stem and seated at the center of the sphere. The sphere was then positioned on the mounting rig, covered with

a plastic sheath, and submerged in the hot water bath until the sphere thermocouple temperature and the water bath thermocouple reached the steady state water bath set point temperature.

3. Once the sphere reached steady state, it was removed from the hot water bath, and the plastic sheath was removed. The ambient temperature and sphere temperatures were recorded at 0.5-second intervals. The process was repeated for the remaining two spheres.

Results

Temperatures at the core as a function of time for the gold plated copper sphere, the black painted copper sphere, and the rubber sphere are presented respectively in Figure 1, Figure 3, and Figure 5. The natural logarithm of the normalized temperature is plotted as a function of time for the same three spheres in Figure 2, Figure 4, and Figure 6. The effective heat transfer coefficients, Biot numbers, and validity or invalidity of the lumped capacitance method for the three spheres are shown in Table 1.

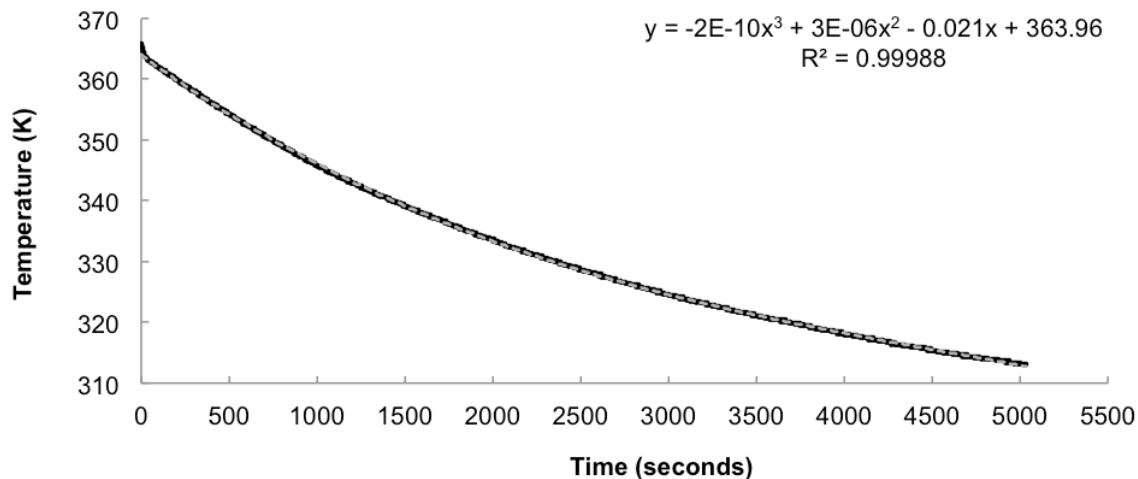


Figure 1. Core temperature as a function of time for the gold plated copper sphere.

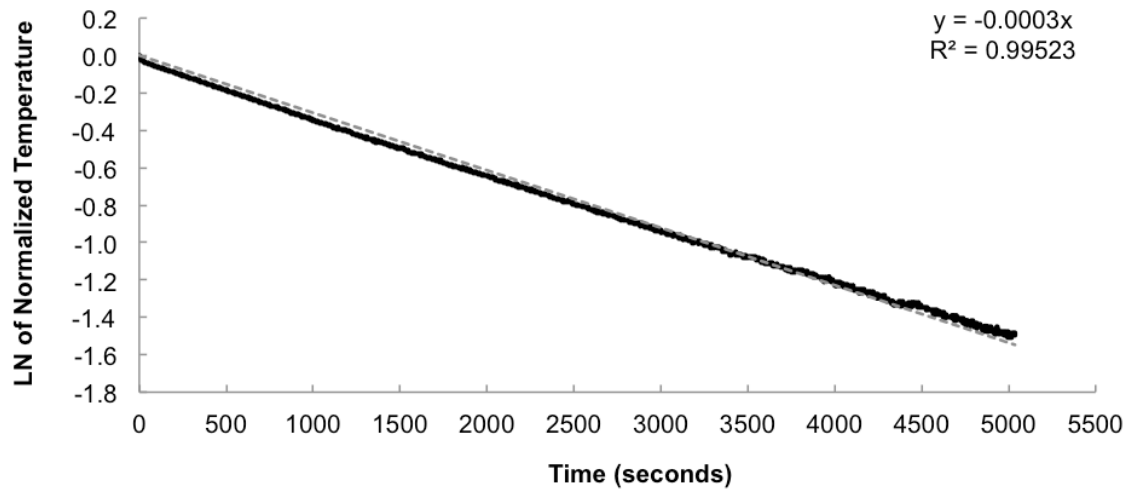


Figure 2. Natural logarithm of the normalized temperature at the core as a function of time for the gold plated copper sphere.

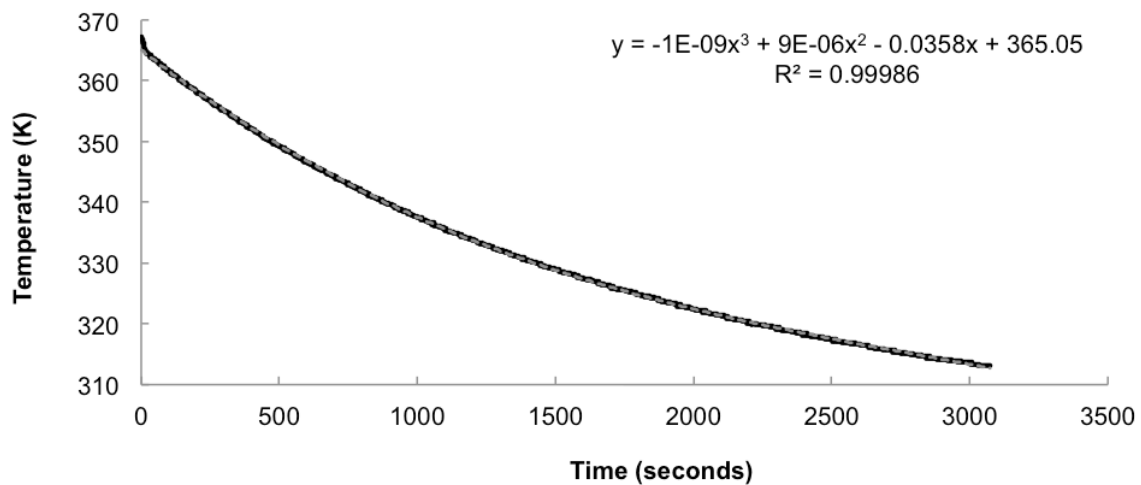


Figure 3. Core temperature as a function of time for the black painted copper sphere.

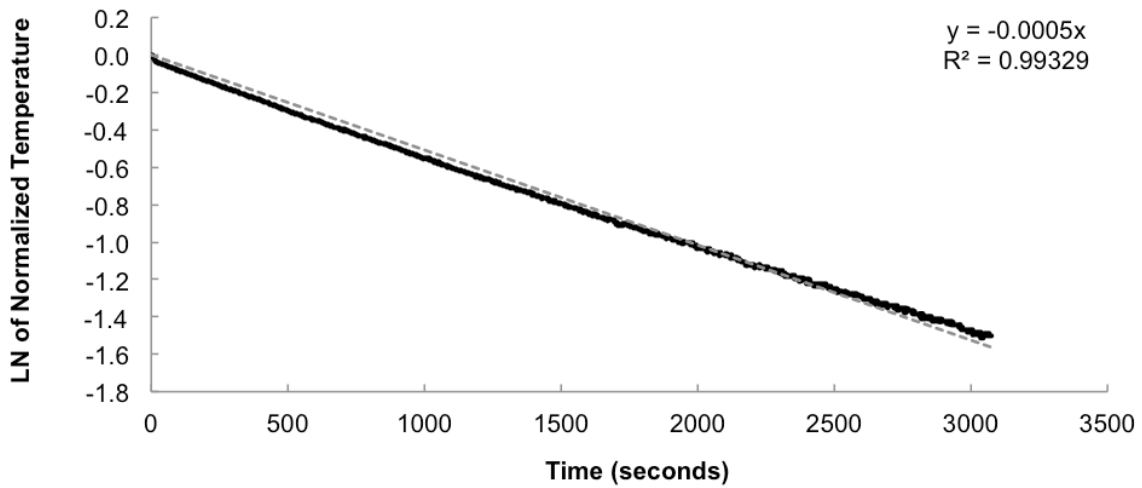


Figure 4. Natural logarithm of the normalized temperature at the core as a function of time for the black painted copper sphere.

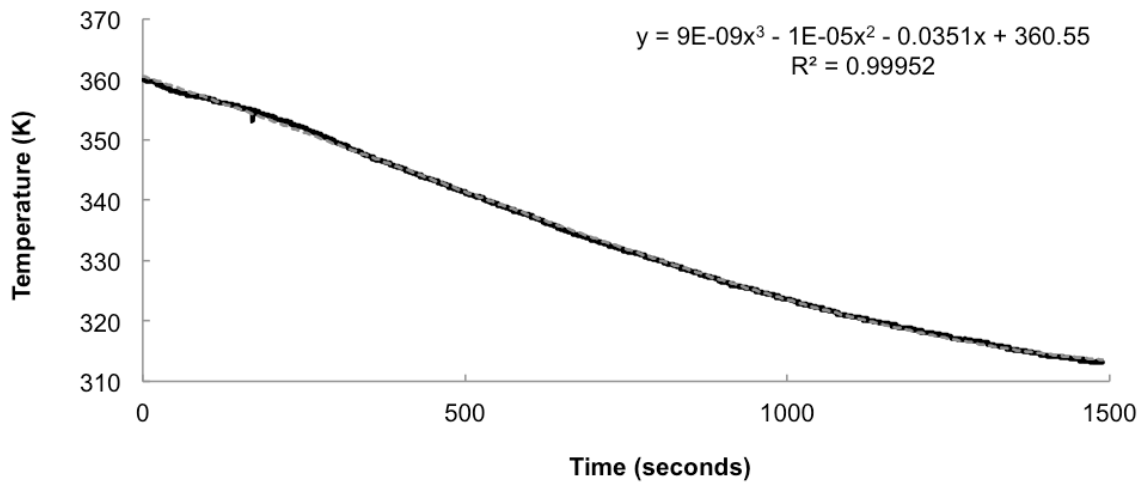


Figure 5. Core temperature as a function of time for the rubber sphere.

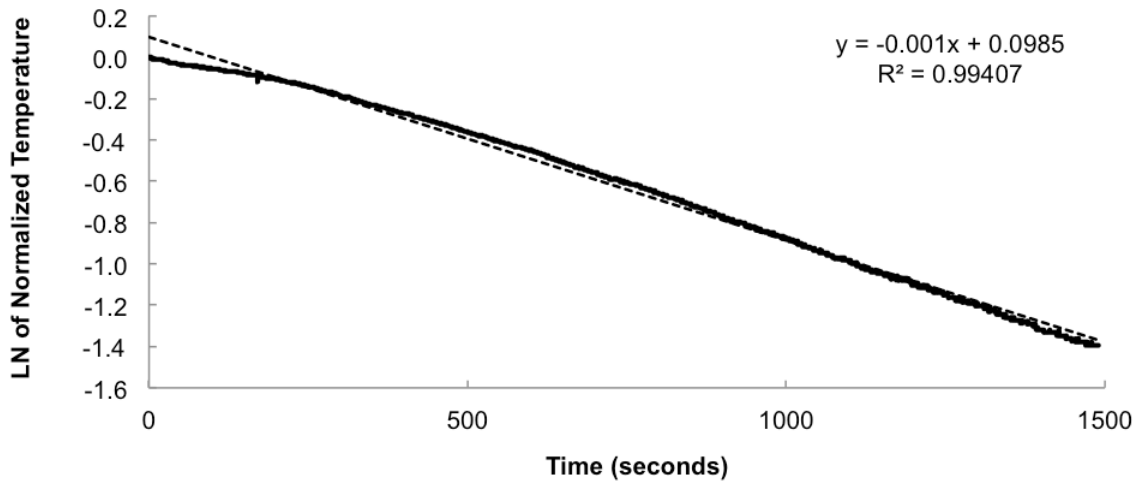


Figure 6. Natural logarithm of the normalized temperature at the core as a function of time for the rubber sphere.

Table 1. Experimentally obtained overall heat transfer coefficient, Biot number, and validity / invalidity of the lumped capacitance method for each sphere.

	Gold Plated Copper Sphere	Black Painted Copper Sphere	Rubber Sphere
Effective Heat Transfer Coefficient (W/m ² -K)	8.7	13.9	11.3 ^A
Biot Number	1.78 x 10 ⁻⁴	2.85 x 10 ⁻⁴	1.51 ^B
Lumped Capacitance Valid (Yes/No)	Yes	Yes	No

- A. A plot of the natural logarithm of normalized temperature versus time is non-linear and yields variable h , with a value of $h_{effective}$ obtained from a line tangent to the curve as shown in Figure 6.
- B. Based on $h_{effective}$ and material properties for the rubber sphere, the Biot number indicates that the lumped capacitance method is not valid.

The empirical natural convection coefficients, Nusselt numbers, and predicted convective heat losses for the gold plated copper sphere are presented respectively in Figure 7, Figure 8, and Figure 9.

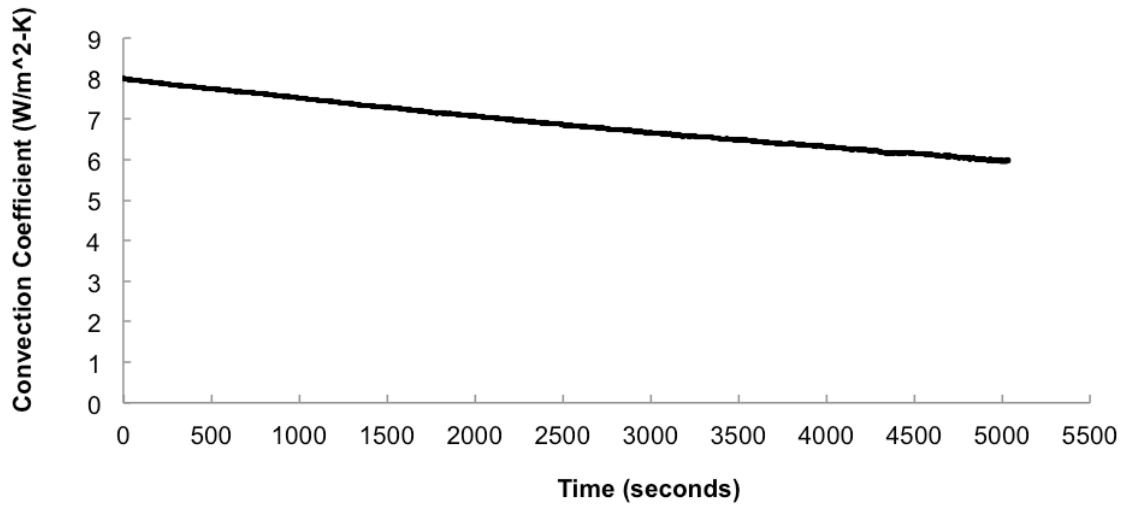


Figure 7. Empirical convection coefficients as a function of time for the gold plated copper sphere.

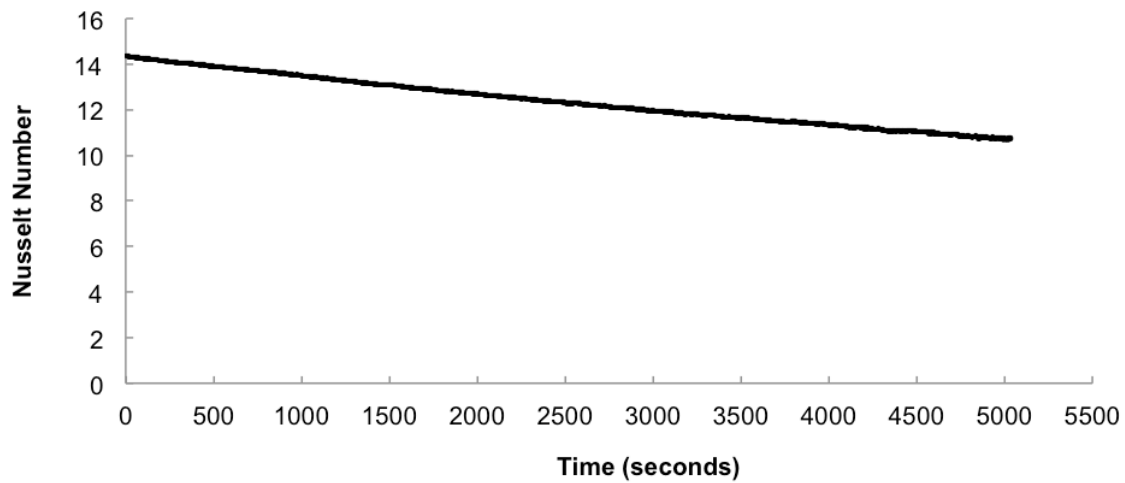


Figure 8. Empirical Nusselt numbers as a function of time for the gold plated copper sphere.

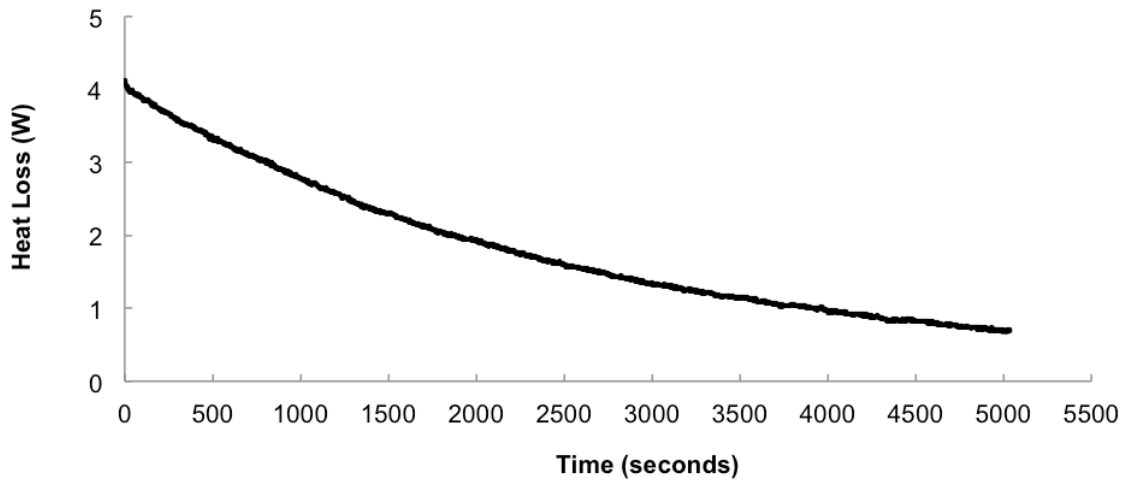


Figure 9. Predicted convective heat loss as a function of time for the gold plated copper sphere.

The empirical natural convection coefficients, Nusselt numbers, and predicted convective heat losses for the black painted copper sphere are presented respectively in Figure 10, Figure 11, and Figure 12.

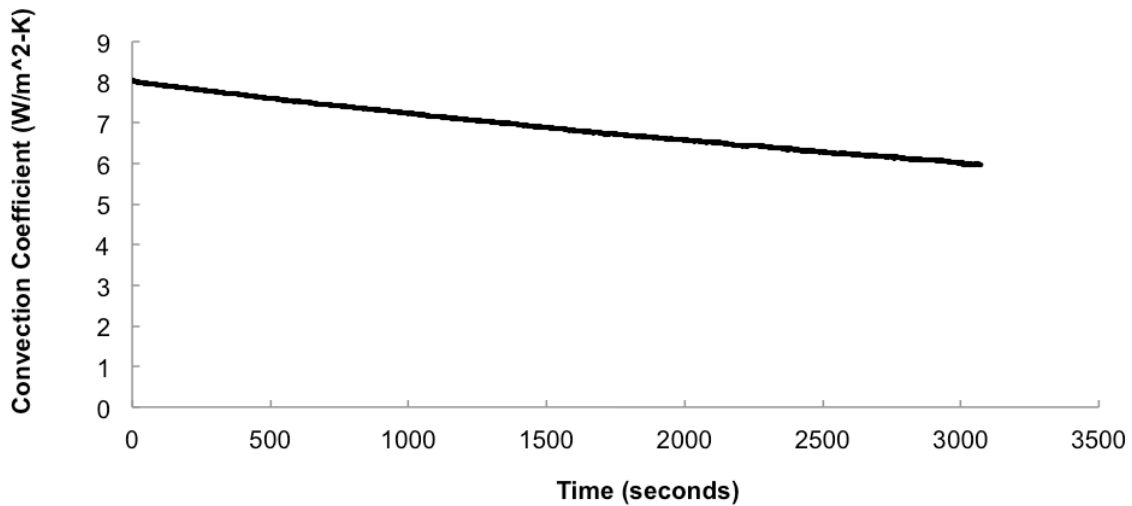


Figure 10. Empirical convection coefficients as a function of time for the black painted copper sphere.

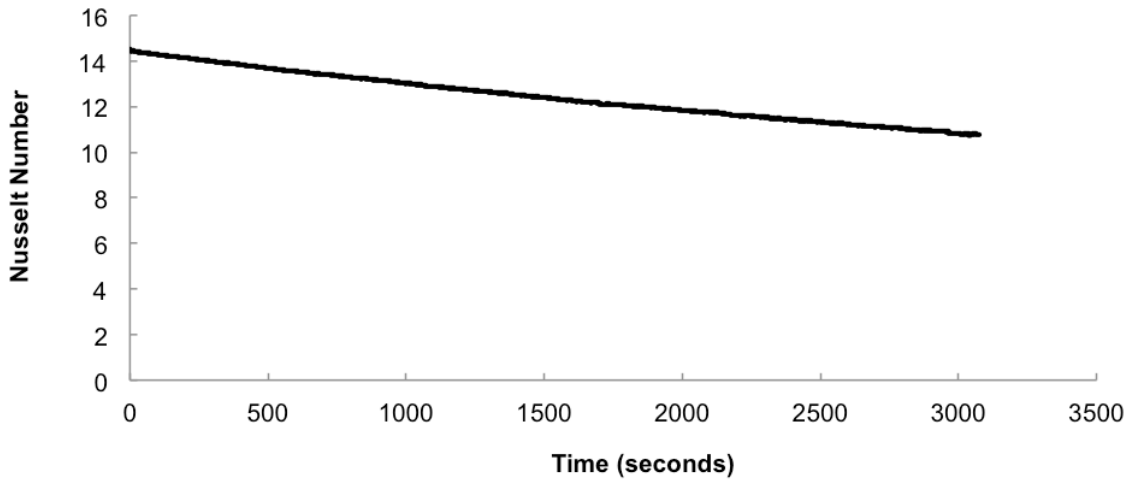


Figure 11. Empirical Nusselt numbers as a function of time for the black painted copper sphere.

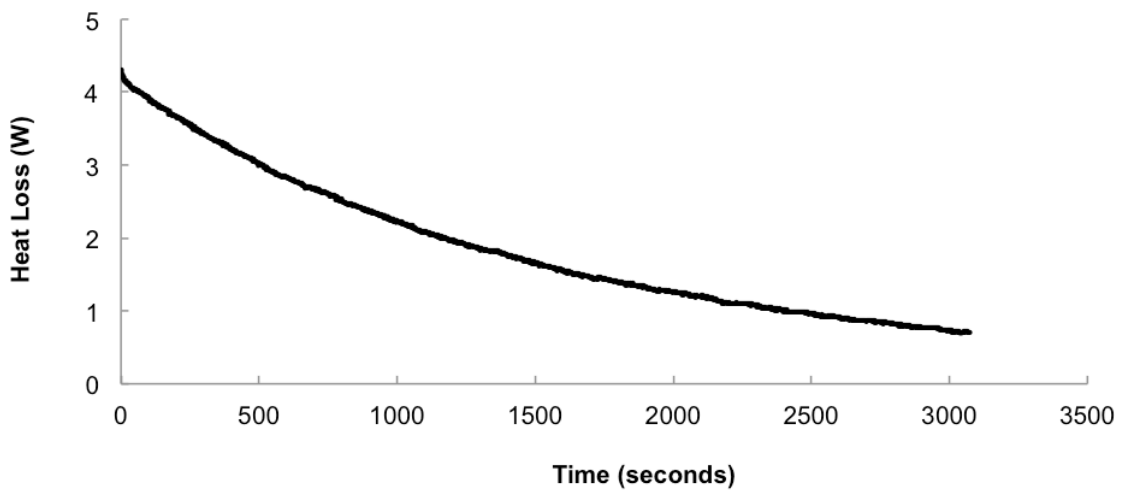


Figure 12. Predicted convective heat loss as a function of time for the black painted copper sphere.

Predicted total heat loss (radiation and convection) and measured total heat loss rates are plotted in Figure 13 for the gold plated copper sphere and in Figure 14 for the black painted copper sphere.

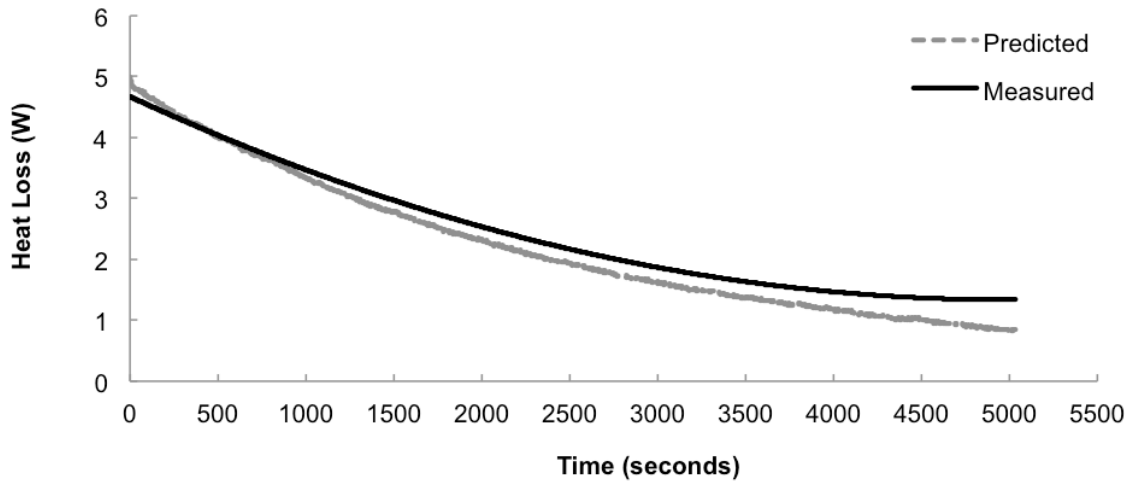


Figure 13. Predicted and measured total heat loss rates as a function of time for the gold plated copper sphere.

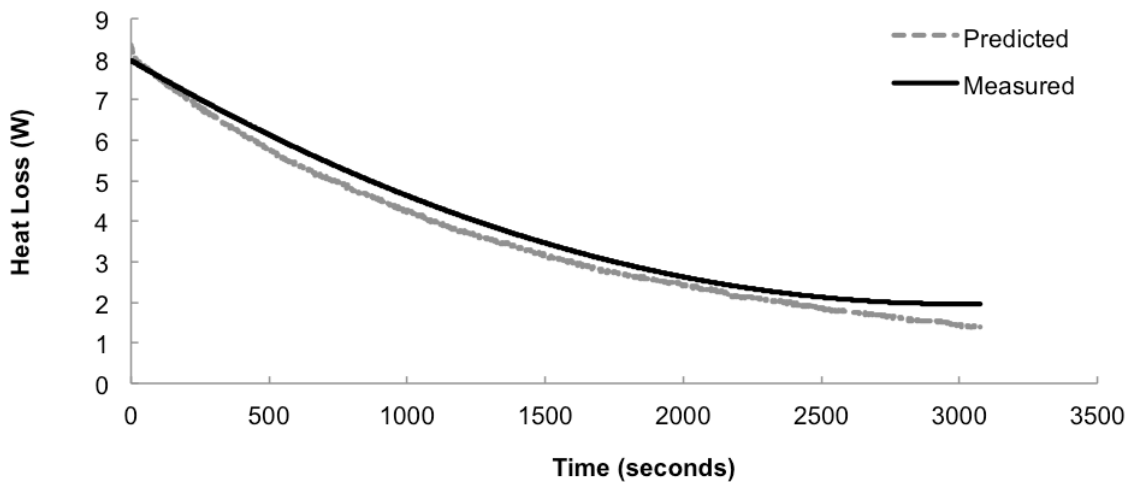


Figure 14. Predicted and measured total heat loss rates as a function of time for the black painted copper sphere.

Discussion

1. Is the lumped capacitance model appropriate? Why or why not?

If the Biot number is less than 0.1, it can be assumed with reasonable accuracy that spatial variations of temperature within the solid are negligible and the lumped capacitance method is valid. As presented in Table 1, the lumped mass model is valid for both the gold plated copper sphere and the black painted copper sphere, as both have Biot numbers much less than 0.1. From Table 1, the lumped mass model is not valid for the rubber sphere, as a corresponding Biot number of 1.51 indicates the conduction resistance is not negligible compared to the convection resistance. Therefore, significant temperature gradients are present within the rubber sphere.

2. The variation of h with time.

For natural convection, the convection coefficient is related to the temperature difference between the sphere surface and ambient temperature. As shown in Equation 6 and Equation 9, the Nusselt number and corresponding convection coefficient are dependent on the Rayleigh number. The Rayleigh number represents the ratio of the buoyant to viscous forces multiplied by the ratio of the momentum to thermal diffusivity. As indicated by the numerator of the Rayleigh number, the buoyant force due to a fluid density gradient is proportional to the temperature difference between the sphere surface and the ambient temperature. Therefore, as this temperature difference and driving potential decay while the sphere approaches an equilibrium state with its surroundings, the convection coefficient must also decay as shown in Figure 7 and Figure 10.

3. Core and surface temperatures during cooling.

The core temperature time history for the gold plated copper sphere, black painted copper sphere, and rubber sphere are presented in Figure 1, Figure 3, and Figure 5, respectively. For the two copper spheres, the center temperature profile is an exponential decay over time that asymptotically approaches the ambient, surrounding temperature. The temperature of the black painted copper sphere decays at a faster rate than the gold plated copper sphere due to the increased effect of radiation heat loss. Since the lumped capacitance model is valid for the two copper spheres, the surface temperature time history would mirror this exponential decay trend with nearly identical temperature magnitudes. The temperature magnitudes are not exactly identical due to the fact that copper has a finite rather than infinite thermal conductivity. Due to its geometry and the material properties of the rubber sphere, its core temperature decays at a faster rate than the two copper spheres, but it also asymptotically approaches the ambient, surrounding temperature. Since the lumped capacitance model is not valid for the rubber sphere, its surface temperature does not directly mirror the magnitude or the trend of the core temperature. To determine the surface

temperature of the rubber sphere, an exact, infinite series solution is needed over the entire time history of the experiment.

4. *The effect of radiation.*

The effect of radiation cannot be neglected and accounts for a significant portion of the total heat loss from both of the copper spheres. The time history of heat loss rates due to convection, radiation, and the total heat loss for the gold plated copper sphere are presented in Figure 15. The convective, radiation and total heat loss rates are plotted in Figure 16 for the black painted copper sphere. For the gold plated copper sphere, the heat loss due to radiation accounts for approximately 17% of the total heat loss with an emissivity value of 0.20. Heat loss due to radiation accounts for approximately 48% of the total heat loss for the black painted copper sphere with an emissivity value of 0.90.

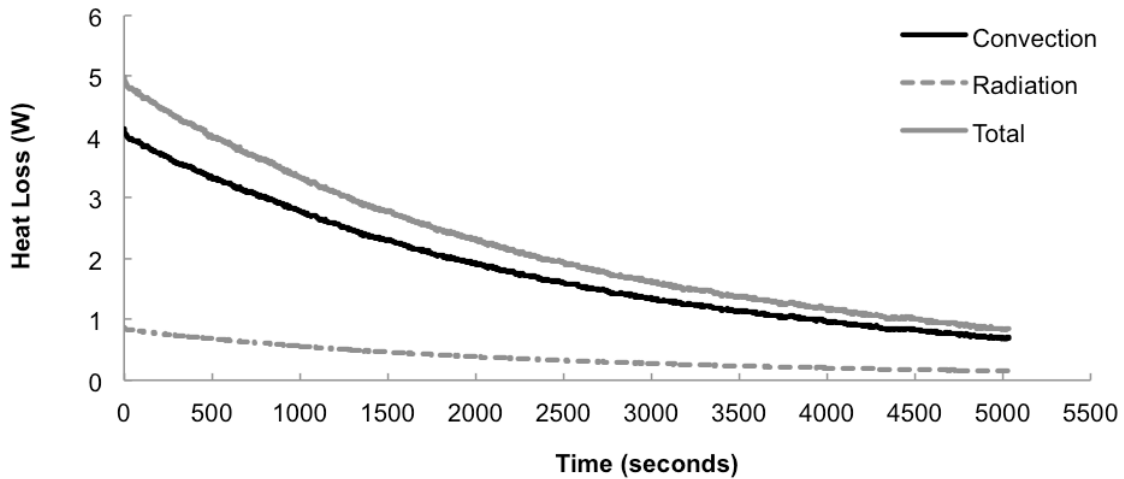


Figure 15. Total heat loss, heat loss due to convection, and heat loss due to radiation as a function of time for the gold plated copper sphere.

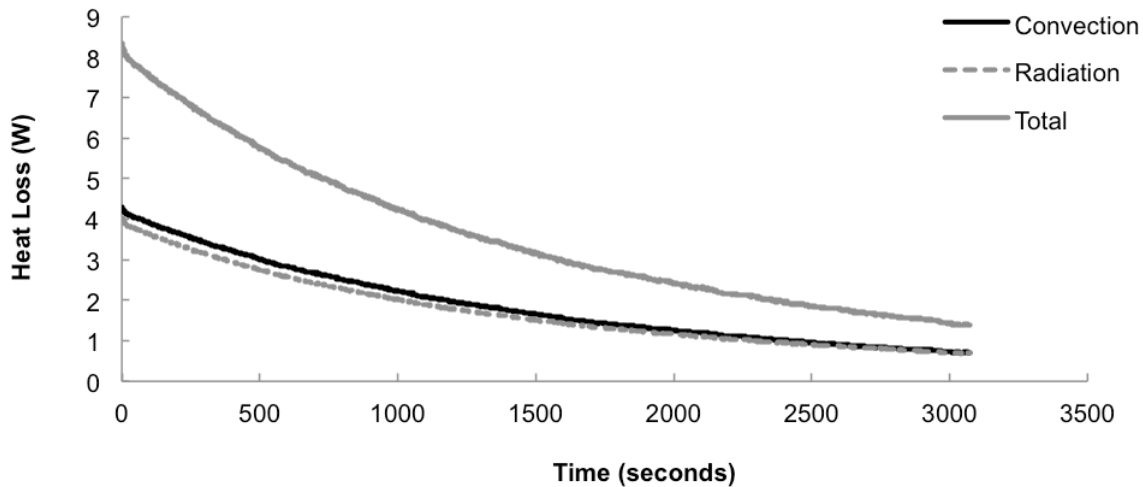


Figure 16. Total heat loss, heat loss due to convection, and heat loss due to radiation as a function of time for the black painted copper sphere.

5. *How reasonable are the emissivity estimates?*

Emissivity values were estimated at 0.20 for the gold plated copper sphere and 0.90 for the black painted copper sphere. There is a large variation in emissivity estimates for gold and gold plating [2]. Emissivity estimates for gold and various platings are dependent on level of polishing, level of oxidation, and application method, with emissivity values as low as 0.02 – 0.04 for highly polished gold plating. A larger emissivity estimate of 0.20 was utilized to account for the recent lack of polishing, defects in the gold plating, and any oil or grease present on the surface of the plating. There is less variation in the emissivity estimates for black paint with an emissivity of 0.90 [2] being within the typical range.

6. *Discuss differences between measured and predicted values of q_{total} .*

Predicted values of the total heat loss rate were on average within 9% of measured values for the gold plated copper sphere, and within 8% for the black painted copper sphere, over the full time history of the experiments. To estimate / predict values of radiation heat losses, emissivity values were assumed for both spheres. As previously discussed, although these values are within the published ranges for each case, the remaining uncertainty in the actual emissivity of each surface is a contributing factor to the difference between measured and predicted heat loss rates. The use of empirical Nusselt number correlations introduces

additional uncertainty of around 20% in predicted convection heat loss rates. In calculating the Rayleigh number, the volumetric thermal expansion coefficient was evaluated at the film temperature at each time step, but the fluid properties were only resolved at the average film temperature with the same average properties utilized over the entire time history. This introduces an additional uncertainty in predicted convection heat loss rates.

Conclusion

The lumped capacitance model for transient conduction was tested for three heated spheres; a gold plated copper sphere, a black painted copper sphere, and a rubber sphere. The assumption was validated for the gold plated copper and the black painted copper spheres, and the lumped capacitance method was used to quantify the total heat loss through natural convection and radiation exchange with the surroundings. The measured heat loss rates were compared to predicted heat losses and were found to be within 9% for the gold plated copper sphere and within 8% for the black painted copper sphere. The differences between predicted and measured total heat losses can be attributed to the use of an empirical correlation for the convection coefficient, the assumed surface emissivity, and the use of fluid properties evaluated at the average film temperature.

References

1. F.P. Incropera et. al., Introduction to Heat Transfer, 6th ed. Hoboken, NJ: Wiley, 2011.
2. Avallone, E. A., Baumeister, T., Sadegh, A. M., and Marks, L. S., 2007, Marks standard handbook for mechanical engineers, McGraw-Hill, New York.